Optical studies on the surface-induced tilted layers in freestanding films of two no-layer-shrinkage liquid crystal compounds

S. T. Wang,* X. F. Han,† Z. Q. Liu, B. K. McCoy, and C. C. Huang
School of Physics and Astronomy, University of Minnesota, Minneapolis, Minnesota 55455, USA
(Received 29 March 2006; published 19 September 2006)

Null transmission ellipsometry has been employed to study the molecular arrangements in freestanding films of two no-layer-shrinkage liquid crystal homologous compounds above the bulk smectic *A*–smectic C^* (Sm C^*) transition temperature. An unusual nonplanar-parallel or nonplanar-antiparallel-parallel transition has been observed in both compounds under a proper electric field. With the addition of one CH_2 group, while the SmC^* phase is more stable thermally, the magnitude of the critical field needed to induce a parallel-antiparallel transition decreases dramatically.

DOI: 10.1103/PhysRevE.74.031707 PACS number(s): 61.30.Gd, 77.84.Nh

I. INTRODUCTION

Since the discovery of no-layer-shrinkage (NLS) behavior through the smectic *A*–smectic C^* (Sm*A*-SmC^*) transition in some liquid crystals, a considerable amount of research effort has been aimed at gaining much better understanding of the related physical properties [1–5]. Additionally this class of compounds also exhibits an anomalous electroclinic effect and low birefringence [6,7]. Having these physical properties, the compounds are found to be extremely promising candidates for various applications in electro-optical switching devices. Thus the problem of carefully characterizing their physical properties is not just academic, it has important technological implications as well. The electroclinic effect above the Sm*A*-SmC^* transition is one of the prominent features associated with this transition, in which a moderate applied electric field (E) can induce measurable molecular tilt. To date, both the NLS behavior and anomalous electroclinic effect can be qualitatively explained by the de Vries diffuse cone model [8]. However, there exists systematic deviation between the experimental data and predictions based on this model. In light of this discrepancy, one microscopic theory has been proposed by Meyer and Pelcovits [9].

Liquid crystal freestanding films have offered a unique sample geometry from which numerous physical properties and molecular arrangements have been acquired experimentally [10–13]. Due to the surface tension, enhanced surface ordering in freestanding films is very common, which yields rich surface phases in some compounds [14,15]. To date, at least three surface structures have been observed in freestanding films above the Sm*A*-SmC^* transition temperature. As illustrated in Figs. 1(a) and 1(b), surface-induced tilted layers on two free surfaces can tilt in the same orientation (parallel) [16,17] or in the opposite orientation (antiparallel) [17–19]. In the nonplanar surface structure as shown in Fig. 1(c), the tilt planes of the two outmost surface layers are different. This kind of structure was first discovered in one NLS compound under a very small electric field [20], and recently observed in one layer-shrinkage compound [21]. Besides the nonplanar structure, some other remarkable results have been found from freestanding films of NLS compounds. One NLS compound with a fluoroether tail has been reported to show a double reentrant transition between parallel and antiparallel surface structures upon cooling under a constant E field [22]. Recent studies on another compound 8O23[78-] (8O) have yielded an unusual surface transition which depends on the strength of the applied electric field [23].

In this paper, we will report detailed null transmission ellipsometry (NTE) studies on two fluoro-containing NLS compounds: 7O23[7F8-] (7O) and 8O [24]. The chemical structures and phase sequences of these two compounds are listed in Fig. 1(d). They are adjacent members of a homologous series differing by one CH_2 group in the alkyl tail. The Sm*A*-SmC^* transition in 8O is about 20 K higher than that of 7O.

The results show a nonplanar-antiparallel-parallel or nonplanar-parallel transition upon cooling for different strengths of E. This behavior exists in both compounds. At some temperatures, increasing E can induce a transition from a parallel to an antiparallel state. The critical field is strongly dependent on the film thickness. With one additional CH_2

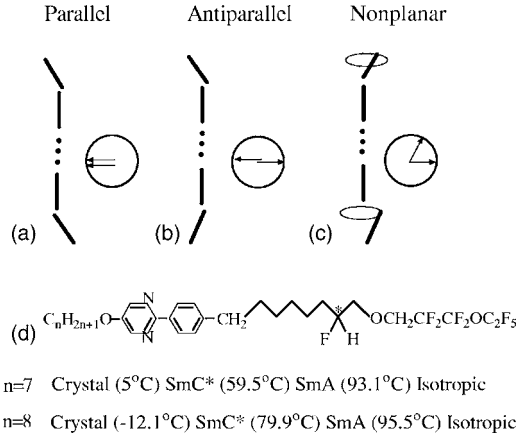

FIG. 1. (a), (b), and (c) show three different surface structures in which the two outmost layers are tilted. (d) shows the chemical structure and bulk phase sequences for compounds 7O23[7F8-] and 8O23[7F8-].

*Present address: NSLS, Brookhaven National Laboratory, Upton, NY 11973.

†Present address: Seagate Technology, Bloomington, MN 55435.

group in 8O, while the SmC^* phase is stable in a much higher temperature window, the critical electric field to induce a parallel-antiparallel transition decreases dramatically. These results are shown in Sec. III. The next section briefly discusses the experimental methods.

II. EXPERIMENTAL METHODS

The liquid crystal freestanding films were prepared in temperature-regulated two-stage ovens filled with helium gas to minimize the sample degradation. The films are pulled across a circular hole in the center of a glass cover slip in the smectic phase of the compounds. In our NTE, the circular hole with a diameter of 4.5 mm was surrounded by eight equally spaced electrodes. By applying specific sets of sinusoidal voltages to the eight electrodes, a uniform and rotatable E can be created in the plane of the film. The variable α denotes the angle between E and the incident plane defined by the incident laser light and the film normal. The maximum strength of the applied electric field is about 45 V/cm.

The details of our NTE experimental setup have been described elsewhere [25]. If the film has net polarization in the film plane, the polarization will align with E. In many cases, the following three experimental runs were conducted on a given freestanding film. First, since E can be rotated through 360° in the film plane, by recording the ellipsometric parameters Δ and Ψ, defined below, at each angle α we can infer the optical symmetry of the phase and obtain the molecular arrangement in the film. Rotations of E are usually done with 24 steps. Second, NTE runs were also performed by ramping the temperature up and down. During the temperature ramp, the direction of E was switched between two orientations in order to see changes in the state. Third, to determine the critical field associated with the parallel-antiparallel transition, the ellipsometric parameters were acquired with varying E field at a constant temperature.

In our ellipsometry system, Δ measures the phase difference between the $\hat{p}$ and $\hat{s}$ components of the incident light necessary to produce linearly polarized transmitted light. Ψ describes the polarization angle of this linearly polarized light. Physically, Ψ represents the effect of the film on the orientation of the polarized light and Δ is related to the biaxiality of the film.

Since the freestanding film geometry is used in our experimental setup, determining the film thickness is always our first goal. If the compound exhibits a uniaxial SmA phase without surface-induced tilt, the indices of refraction (n_o, n_e) and the layer thickness (d) can be determined accurately by pulling a series of films in this uniaxial SmA phase using NTE system. At the same time, the number of layers of the film can also be determined. This method is described in [17].

III. EXPERIMENTAL RESULTS AND DISCUSSION

Figures 2(a) and 2(b) show Δ and Ψ as functions of temperature from a ten-layer film of 7O upon cooling under E =40 and 22 V/cm, respectively. Under a larger field (E =40 V/cm), three transitions can be identified at 70.7 °C (T_1), 69.2 °C (T_2), and 66.4 °C (T_3) in Fig. 2(a). Above T_1, the film is in the uniaxial SmA phase with no tilted surface layers. The parameters Δ and Ψ acquired at α=90° are equal to Δ and Ψ obtained at α=270°. At T_1, the surface layers begin to tilt and there is a difference between Δ_{90} and Δ_{270}. As the temperature decreases further, near T_2, $\Delta_{90}-\Delta_{270}\approx 0$ while $\Psi_{270}-\Psi_{90}$ continues to increase. At T_3, $\Delta_{90}-\Delta_{270}$ suddenly increases and $\Psi_{270}-\Psi_{90}$ suddenly decreases.

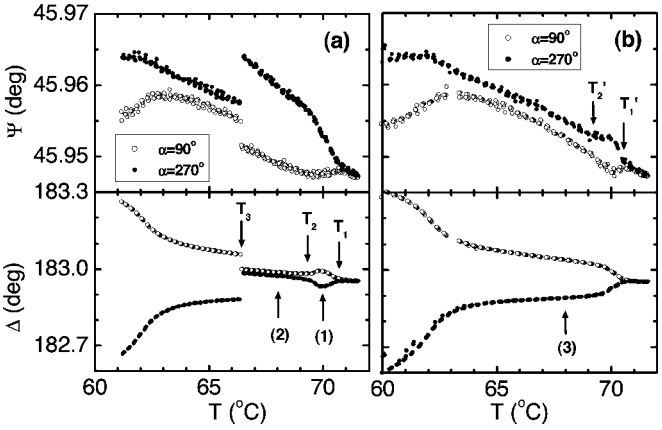

FIG. 2. Temperature dependence of Δ and Ψ obtained upon cooling under two opposite directions of E from a ten-layer film of 7O with E= (a) 40 and (b) 22 V/cm. Open circles and solid dots are data obtained under α=90° and 270°, respectively. In (a), three downward arrows located at T_1=70.7 °C, T_2=69.2 °C and T_3 =66.4 °C indicate three transition temperatures. In (b), two downward arrows at T_1'=70.7 °C and T_2'=69.2 °C show two transition temperatures. Three upward arrows labeled with numbers indicate three temperatures at which rotation data are obtained and shown in Fig. 4 below.

According to previous experimental results [11,17,23], such data suggest that an antiparallel structure forms between T_2 and T_3 and a parallel structure forms below T_3. The structure between T_1 and T_2 is a nonplanar structure, different from both parallel and antiparallel structures. When the applied field is smaller (E=22 V/cm), a continuous transition happens at T_2' (69.2 °C), shown in Fig. 2(b). The structure below T_2' is parallel. Between T_1' (70.7 °C) and T_2', the film has the nonplanar structure. The transitions at T_2 and T_2' are continuous and different from the first-order transition at T_3.

Figure 3 displays Δ and Ψ as functions of temperature upon cooling and heating from a ten-layer film of 8O. It shows that three surface structures also exist in the ten-layer film of 8O. No hysteresis is observed through the nonplanar-antiparallel transition within the experimental resolution as shown in Fig. 3. However, there is a noticeable thermal hysteresis associated with the antiparallel-parallel transition, which is demonstrated to be a first-order transition.

In order to confirm the three surface structures, rotations of E at different temperatures were performed. Such data at three conditions from a ten-layer film of 7O are given in Fig. 4. In this figure, curves a and b show the data acquired under E=40 V/cm at 70.0 and 68.0 °C, respectively. The data obtained at 68.0 °C under E=22 V/cm are plotted in Fig. 4 as curve c. Curve c is concave downward with a wide span in Δ, which is the main feature of a parallel structure. Curve b

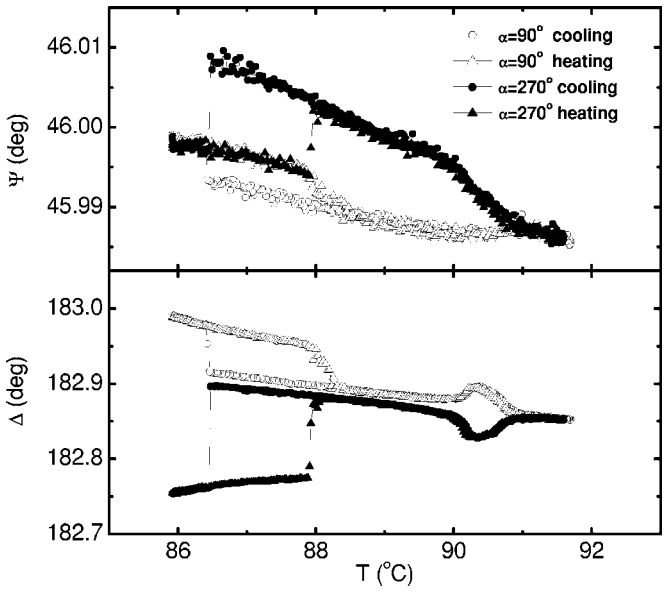

FIG. 3. Ψ and Δ as functions of temperature for a ten-layer film of 8O under $E=22$ V/cm with $\alpha=90°$ (open symbols) and 270° (solid symbols) upon cooling (circles) and heating (triangles). The ramping rate was 40 mK/min.

is concave right with a large span in Ψ, which is characteristic of an antiparallel structure. Curve *a* does not display either of these features, yielding a nonplanar structure. Such plots demonstrate that the surface layers form three distinct structures under these three conditions.

To model these three surface structures, simulations of Δ and Ψ under rotations of E are conducted by using the 4 ×4 matrix method [26]. Each layer in the freestanding film is modeled as a uniaxial slab with extraordinary index of refraction (n_e) along $\hat{n}$ and ordinary index of refraction (n_o) along the other two principal axes. The indices of refraction and the layer spacing (d) are determined by pulling thirty 7O films at 73.5 °C where there are no tilted surface layers [17]. Simulations are then implemented using the measured values $n_e=1.514\pm0.005$, $n_o=1.427\pm0.005$, and $d=38.4\pm0.5$ Å.

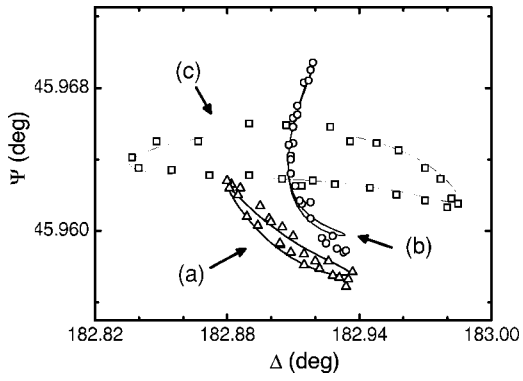

FIG. 4. Ψ versus Δ data and simulation results. Curves *a* and *b* show the data acquired at 70.0 and 68.0 °C with $E=40$ V/cm, respectively. Curve *c* shows the data obtained at 68.0 °C with $E=22$ V/cm. Curves *a*, *b*, and *c* correspond to 1, 2, and 3 in Fig. 2, respectively. Symbols are the data and the solid lines are simulation results.

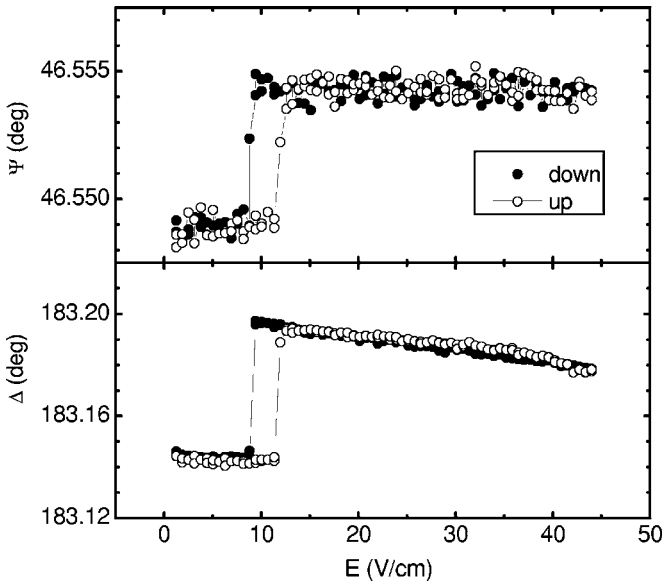

FIG. 5. E scans from a 13-layer film of 7O at 69.2 °C. The open circles and solid dots are the data for ramping E up and down, respectively.

The simulation results are shown as solid lines in Fig. 4. For simplicity, only the two outermost surface layers are assumed to be tilted. From simulation results, the tilt angle of the surface layers in Fig. 4 from *a* to *c* is 6.7°, 7.1°, and 7.1°, respectively. The surface tilt angle increases upon cooling as expected [16]. The small magnitude of the surface tilts justifies the assumption that only the outermost layers are tilted. The molecules in the two surface layers at 70.0 °C have a difference in azimuthal angle of 104°. The continuous evolution of Δ versus α as a function of temperature from the nonplanar structure to the antiparallel or parallel structure has been qualitatively described by polarization evolution [23].

As curves *b* and *c* in Fig. 4 show, increasing E can induce a parallel-antiparallel transition at constant temperature. We performed E scans at different temperatures to explore the field and temperature dependence of the parallel-antiparallel transition. However, for a ten-layer film the critical field (E_c) to induce an antiparallel-parallel transition is close to the limit of E (45 V/cm) in our experimental setup. In addition, there is a large electric field hysteresis associated with the transition as shown in the following. We cannot get a complete picture of this transition for a ten-layer film. We did the E scans for a 13-layer film because we know E_c decreases as the thickness of film increases. The E field was ramped up and down at $\alpha=270°$ at a series of temperatures separated by 0.25 K per step. A typical E scan is shown in Fig. 5. From the jump of Δ or Ψ, the critical field is found. At some temperatures, the E_c could not be identified while decreasing E even when E approached zero [27]. Thus, some data of E_c are missing for ramping E down.

The phase diagram from a 13-layer film is plotted in Fig. 6. As the temperature decreases, the critical field E_c obtained by ramping E up increases generally while E_c obtained by ramping E down decreases first and then increases. The basic features of this phase diagram are similar to the phase dia-

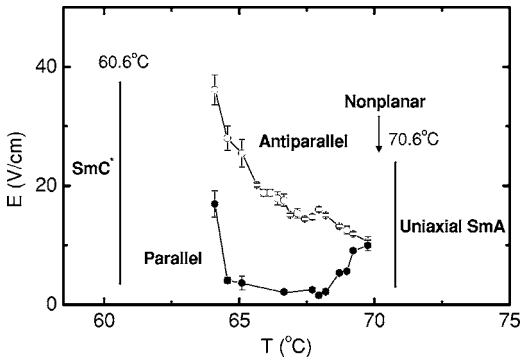

FIG. 6. Phase diagram for 13-layer films of 7O. Open and solid circles are results from ramping E up and down, respectively. Solid lines connecting symbols (above which molecules adopt an antiparallel structure) are guides to the eye. The two vertical solid lines at 70.6 and 60.6 °C separate three temperature windows.

gram obtained from a ten-layer film of 8O [23]. However, there is a large electric field hysteresis associated with the parallel-antiparallel transition in 7O. Moreover, another important difference in the results between 7O and 8O is that the critical field for 7O is larger than that for 8O for films with the same number of layers. For example, for a ten-layer film, 7O needs ~40 V/cm to induce the parallel-antiparallel transition while 8O needs ~22 V/cm.

From Fig. 6, around $E=8.9$ V/cm we may expect a nonplanar-parallel-antiparallel-parallel reentrant transition. Because of the large field hysteresis we could not observe this transition in the 13-layer film of 7O. However, we observed the trend of this surface transition in a ten-layer film of 8O. Figure 7 shows this expected transition under $E=16.3$ V/cm for a ten-layer film of 8O. The jumps of Δ and Ψ at $T_4=90.4$ °C indicate that the transition is a first-order parallel-antiparallel transition. For the parallel structure

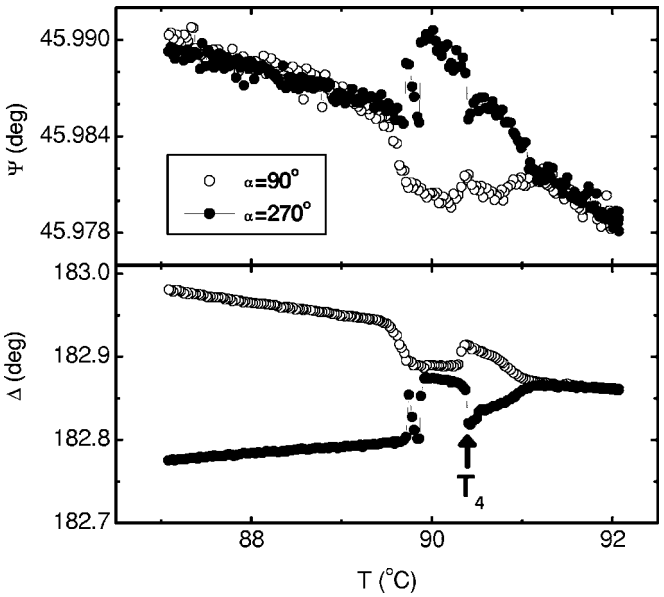

FIG. 7. Ψ and Δ as a function of temperature for ten-layer films of 8O under $E=16.3$ V/cm at $\alpha=90°$ (circles) and 270° (dots) at a cooling rate of 40 mK/min.

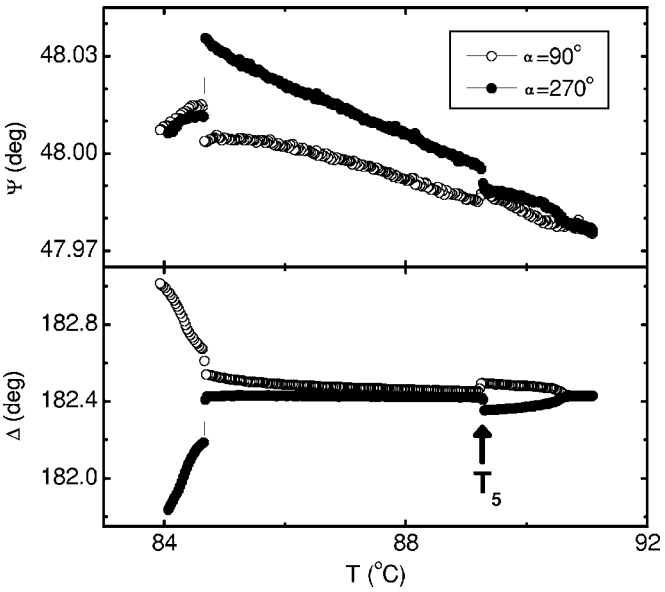

FIG. 8. Ψ and Δ as a function of temperature for 22-layer films of 8O under $E=1.8$ V/cm at $\alpha=90°$ (circles) and 270° (dots) at a cooling rate of 50 mK/min.

shown in Fig. 2, $\Psi_{90} \approx \Psi_{270}$. Figure 7 shows the trend that Ψ_{90} increases and Ψ_{270} decreases in order to make $\Psi_{90} \approx \Psi_{270}$ as the temperature approaches T_4 from above. However, before the difference in azimuthal angle of the two surface layers continuously decreases to 0° to form the parallel structure, it suddenly changes to 180° to become the antiparallel structure which gives sudden changes of both Ψ and Δ. This transition is even more pronounced in a 22-layer film under $E=1.8$ V/cm as shown in Fig. 8, in which $\Psi_{90} \approx \Psi_{270}$ at T_5.

Many films of 20 different thicknesses (N) have been studied for both compounds. The results from thinner films ($N \leq 8$) are similar to Fig. 2(b), with no antiparallel structures observed under the largest field available in our setup (≃45 V/cm). From thicker films ($N>8$), three surface structures have all been observed under appropriate fields. The critical field E_c that induces the parallel-antiparallel transition decreases as the film thickness increases. In previous studies, Chao *et al.* have reported that increasing the electric field can induce a transition from antiparallel to parallel [28]. Their thickness dependence of E_c is similar to our case. Moreover, as the thickness increases, the temperature window for the antiparallel structure decreases. Eventually, in thick films, all the surfaces show parallel states. If we think of N as a parameter, a parallel-antiparallel-parallel transition can be expected as N increases.

In chiral smectic liquid crystals, two types of polarization are possible due to molecular orientations of surface layers: ferroelectric polarization (P_{fe}) and flexoelectric polarization (P_{fl}). Due to chirality, P_{fe} is perpendicular to the tilted plane, and flexoelectric polarization P_{fl} is along the tilt direction. It is generally believed that coupling between P_{fe} or P_{fl} and E is the main driving force in forming surface structures [18,19,29]. When $P_{fl} > P_{fe}$ (or $P_{fl} < P_{fe}$), under an applied E the surfaces of the film will favor antiparallel (or parallel)

structure [19]. If P_{fe} is larger than the in-plane component of P_{fl}, the surfaces can be switched to be parallel by a sufficiently large electric field [18]. Several research groups have reported that the antiparallel-parallel transition can be induced by increasing E [18,28]. On the other hand, because P_{fl} is usually smaller than P_{fe} in chiral liquid crystals the parallel-antiparallel transition is relatively rarely observed. Thus, some other factors should be taken into account, i.e., polarization fluctuations at the two surfaces [17] and elastic energy due to spatial variations of molecules. The nonplanar-parallel or nonplanar-antiparallel-parallel surface transitions have only been observed in NLS compounds so far. These unusual transitions may be unique for NLS compounds. If the de Vries diffuse cone model is correct for the SmA phase of NLS compounds [8], the elastic energy due to spatial variations of molecules should play an important role in the surface transitions of freestanding films of NLS compounds. Further theoretical work needs to be advanced to explain these nonplanar-parallel and nonplanar-antiparallel-parallel surface transitions.

Since at sufficiently large field all the molecules will tilt in the same orientation, it is understandable that the antiparallel-parallel transition happens upon increasing E. For a given film of these two NLS compounds, we may expect a parallel-antiparallel-parallel reentrant transition as E increases.

Because of the one additional CH_2 group, the critical field in 8O is about half of that in 7O for the same film thickness. The layer spacing of 8O is a little bit larger than that of 7O. Thus it is understandable that one additional CH_2 group will have the same effect as the film thickness on the critical field. However, the zigzag shape of the hydrocarbon chain in the alkyl tail may also have some effect as one additional CH_2 group is added.

Another point we should pay attention to is that 8O shows much higher SmA-SmC^* transition (~20 K higher) than 7O does while they have about the same isotropic-SmA transition temperature. This indicates that thermally the SmC^* phase with parallel structure of 8O is more stable than 7O. However, in freestanding films under an applied E field, the parallel structure of 8O is less stable than 7O. More work is needed to address the stability of the parallel arrangement under thermal and electric field effects.

Johnson *et al.* have reported that the surface structures depend on four parameters: temperature, film thickness, electric field, and polarization [17]. Because 7O and 8O are the adjacent members of a homologous series, their polarization should be similar. Thus, for a given film of these two compounds, T, E, and N should be the three parameters that determine the surface structure of the film. In our studies, when one of the three parameters varies monotonically while the other two parameters remain constant, we can get a parallel-antiparallel-parallel reentrant transition. Therefore, we may expect that the antiparallel state occupies an enclosed space in the three-parameter space of T, E, and N. This observation hints that the free energy of this system will have a local minimum in this enclosed space which favors the antiparallel state.

In summary, we have observed a nonplanar-antiparallel-parallel or nonplanar-parallel transition upon cooling from two no-layer-shrinkage compounds. The transition from nonplanar to antiparallel (or parallel) is found to be continuous. We also observed that the surface structure strongly depends on the temperature, electric field, and film thickness. An additional CH_2 group dramatically affects the critical field necessary to induce the parallel-antiparallel transition.

ACKNOWLEDGMENTS

The research was supported in part by the donors of the Petroleum Research Fund, administered by the American Chemistry Society and the National Science Foundation, Solid State Chemistry Program under Grant No. DMR-0106122. Both liquid crystal compounds were kindly provided by 3M, St. Paul, MN.

[1] M. D. Radcliffe, M. L. Brostrom, K. A. Epstein, A. G. Rappaport, B. N. Thomas, R. Shao, and N. A. Clark, Liq. Cryst. **26**, 789 (1999).
[2] F. Giesselmann, P. Zugenmaier, I. Dierking, S. T. Lagerwall, B. Stebler, M. Kašpar, V. Hamplová, and M. Glogarová, Phys. Rev. E **60**, 598 (1999).
[3] J. P. F. Lagerwall, F. Giesselmann, and M. D. Radcliffe, Phys. Rev. E **66**, 031703 (2002).
[4] N. A. Clark, T. Bellini, R.-F. Shao, D. Coleman, S. Bardon, D. R. Link, J. E. Maclennan, X.-H. Chen, M. D. Wand, D. M. Walba, P. Rudquist, and S. T. Lagerwall, Appl. Phys. Lett. **80**, 4097 (2002).
[5] M. Krueger and F. Giesselmann, Phys. Rev. E **71**, 041704 (2005).
[6] M. S. Spector, P. A. Heiney, J. Naciri, B. T. Weslowski, D. B. Holt, and R. Shashidhar, Phys. Rev. E **61**, 1579 (2000).
[7] J. V. Selinger, P. J. Collings, and R. Shashidhar, Phys. Rev. E **64**, 061705 (2001).
[8] A. de Vries, Mol. Cryst. Liq. Cryst. Lett. **49**, 179 (1979).
[9] R. B. Meyer and R. A. Pelcovits, Phys. Rev. E **65**, 061704 (2002).
[10] C. Y. Young, R. Pindak, N. A. Clark, and R. B. Meyer, Phys. Rev. Lett. **40**, 773 (1978).
[11] Ch. Bahr and D. Fliegner, Phys. Rev. Lett. **70**, 1842 (1993).
[12] D. R. Link, J. E. Maclennan, and N. A. Clark, Phys. Rev. Lett. **77**, 2237 (1996).
[13] P. M. Johnson, D. A. Olson, S. Pankratz, T. Nguyen, J. Goodby, M. Hird, and C. C. Huang, Phys. Rev. Lett. **84**, 4870 (2000).
[14] Ch. Bahr, Int. J. Mod. Phys. B **8**, 3051 (1994).
[15] T. Stoebe and C. C. Huang, Int. J. Mod. Phys. B **9**, 2285 (1995).
[16] S. Heinekamp, R. A. Pelcovits, E. Fontes, E. Y. Chen, R. Pindak, and R. B. Meyer, Phys. Rev. Lett. **52**, 1017 (1984).
[17] P. M. Johnson, D. A. Olson, S. Pankratz, Ch. Bahr, J. W. Goodby, and C. C. Huang, Phys. Rev. E **62**, 8106 (2000).

[18] D. R. Link, G. Natale, N. A. Clark, J. E. Maclennan, M. Walsh, S. S. Keast, and M. E. Neubert, Phys. Rev. Lett. **82**, 2508 (1999).
[19] P. O. Andreeva, V. K. Dolganov, C. Gors, R. Fouret, and E. I. Kats, Phys. Rev. E **59**, 4143 (1999).
[20] X. F. Han, D. A. Olson, A. Cady, D. R. Link, N. A. Clark, and C. C. Huang, Phys. Rev. E **66**, 040701(R) (2002).
[21] B. K. McCoy, Z. Q. Liu, S. T. Wang, V. P. Panov, J. K. Vij, J. W. Goodby, and C. C. Huang, Phys. Rev. E **73**, 041704 (2006).
[22] X. F. Han, S. T. Wang, A. Cady, M. D. Radcliffe, and C. C. Huang, Phys. Rev. Lett. **91**, 045501 (2003).
[23] S. T. Wang, X. F. Han, Z. Q. Liu, A. Cady, M. D. Radcliffe, and C. C. Huang, Phys. Rev. E **68**, 060702(R) (2003).
[24] The layer spacing of these two compounds has been measured using small angle x-ray scattering. The results confirmed that they belong to the no-layer-shrinkage compounds since the layer contraction is $<1\%$ from the Sm*A* to SmC^* phase. M.D. Radcliffe (private communication).
[25] D. A. Olson, X. F. Han, P. M. Johnson, A. Cady, and C. C. Huang, Liq. Cryst. **29**, 1521 (2002).
[26] D. W. Berreman, J. Opt. Soc. Am. **62**, 502 (1972); H. Wöhler, G. Haas, M. Fritsch, and D. A. Mlynski, J. Opt. Soc. Am. A **5**, 1554 (1988).
[27] We could decrease E to negative values. However, the negative values mean the electric field direction changes by 180°.
[28] C. Y. Chao, C. R. Lo, P. J. Wu, Y. H. Liu, D. R. Link, J. E. Maclennan, N. A. Clark, M. Veum, C. C. Huang, and J. T. Ho, Phys. Rev. Lett. **86**, 4048 (2001).
[29] R. B. Meyer, Phys. Rev. Lett. **22**, 918 (1969).